**Steel and Composite Structures**, *Vol. 32, No. 5 (2019) 571-582*
DOI: https://doi.org/10.12989/scs.2019.32.5.571


# Feasibility study on the wide and long 9%Ni steel plate for use in the LNG storage inner tank shell

Myungjin Chung [1], Jongmin Kim [2] and Jin-Kook Kim*[3]

[1] *Material and Structure Research Group, POSCO E&C, 241, Incheon tower-daero, Yeonsu-gu, Incheon 22009, Republic of Korea*
[2] *Steel Structure Research Group, POSCO, 100, Songdogwahak-ro, Yeonsu-gu, Incheon 21985, Republic of Korea*
[3] *Department of Civil Engineering, Seoul National University of Science and Technology, 232 Gongneung-ro, Nowon-gu, Seoul 01811, Republic of Korea*

(*Received February 13, 2019, Revised August 24, 2019, Accepted August 26, 2019*)

**Abstract.** This study aimed to assess the feasibility on the wide and long 9%Ni steel plate for use in the LNG storage inner tank shell. First, 5-m-wide and 15-m-long 9%Ni steel plates were test manufactured from a steel mill and specimens taken from the plates were tested for strength, toughness, and flatness to verify their performance based on international standards and design specifications. Second, plates with a thickness of 10 mm and 25 mm, a width of 4.8~5.0 m, and a length of 15 m were test fabricated by subjecting to pretreatment, beveling, and roll bending resulting in a final width of 4.5~4.8 m and a length of 14.8m with fabrication errors identical to conventional plates. Third, welded specimens obtained via shield metal arc welding used for vertical welding of inner tank shell and submerged arc welding used for horizontal welding were also tested for strength, toughness and ductility. Fourth, verification of shell plate material and fabrication was followed by test erection using two 25-mm-thick, 4.5-m-wide and 14.8-m-long 9%Ni steel plates. No undesirable welding failure or deformation was found. Finally, parametric design using wide and long 9%Ni steel plates was carried out, and a simplified design method to determine the plate thickness along the shell height was proposed. The cost analysis based on the parametric design resulted in about 2% increase of steel weight; however, the construction cost was reduced about 6% due to large reduction in welding work.

**Keywords:** LNG storage inner tank shell; 9%Ni steel; wide and long plate; fabrication; erection; cost analysis

## 1. Introduction

LNG represents the liquefied natural gas, which is mainly composed of methane along with ethane and nitrogen. It is cooled down to approximately –162°C for storage and transport under non-pressurized conditions. It is generally imported in a dedicated vessel and stored in a storage tank at LNG production base before it is vaporized and transmitted to power plants or city gas pipelines. The use of LNG, as an eco-friendly fuel, has increased rapidly in automobiles, ships, and power plants. Consequently, the storage and production facilities of LNG are increasing in the Middle East countries for export and Asian countries such as South Korea for import (IGU 2017). The safe and economic design and construction of the structures has prompted several studies involving inner (CLP Power 2006, Nishigami *et al*. 2012, Khamehchi *et al*. 2013, Panchal and Soni 2014, Yang and Yang 2014, Bouknight 2015, Lee *et al*. 2016b, Sun *et al*. 2019) and outer tanks (Hoyle *et al*. 2013, Hjorteset *et al*. 2013, ARUP 2017).

The LNG storage tank consists of an inner tank that directly stores the liquid and an outer tank that forms an additional barrier. Depending on the storage level of the liquid and vapor in the inner and outer tanks, the tank type is categorized into single containment, double containment, full containment, and membrane. It is re-divided into above-ground and in-ground storage tanks depending on its installation location (Bouknight 2015). Basically, the safety level of the full containment tank is higher than that of the single or double containments. Though the membrane is reported to show similar safety (Lee *et al*. 2016a), lack of practical application has led to the market dominance of the full containment tank. The above-ground tank with full containment is generally designed and constructed due to its shorter construction period and better disposal conditions after lifetime compared with the in-ground tank (CLP Power 2006).

The construction of full containment tank is consisted of following representative works, (1) pile foundation; (2) bottom concrete slab; (3) prestressed concrete wall and reinforced concrete roof; (4) bottom, wall and roof vapor barrier with ASTM A516 (2017) carbon steel plate; and (5) inner tank with 9% Ni steel plates.

Recently, the market is rapidly changing, and the demand for shortening the construction period is becoming high because the shorter construction time could allow earlier production and result in earlier revenue generation. The construction period is a very important factor in selecting the construction company.

As shown in a typical construction schedule of full containment tank of Fig. 1, it takes about 30 months to complete the structure, and critical path is found in inner shell which requires about 10 months. The inner tank shell

*Corresponding author, Ph.D., Professor,
E-mail: jinkook.kim@seoultech.ac.kr


http://www.techno-press.org/?journal=scs&subpage=6
ISSN: 1229-9367 (Print), 1598-6233 (Online)

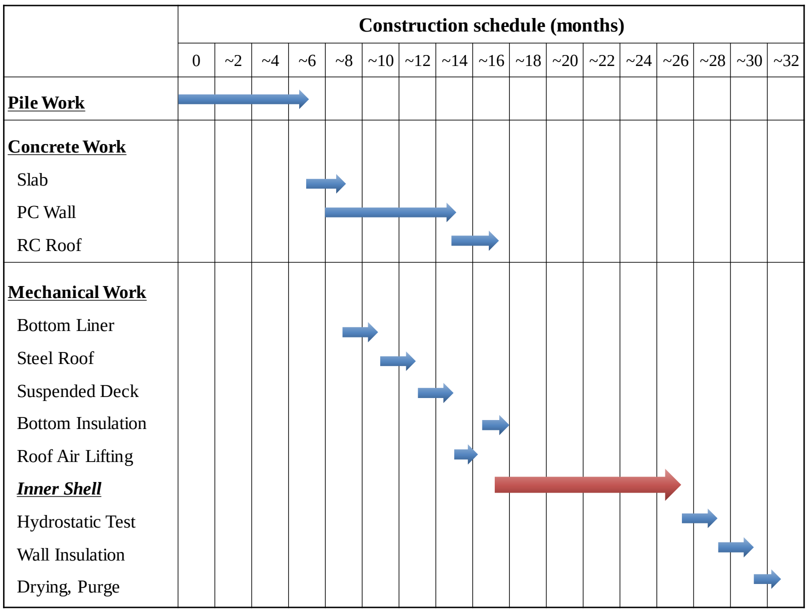


Fig. 1 Typical construction schedule of 160,000 $m^3$ full containment tank (Bouknight 2015)

is assembled in a circumferential direction with 3.6~4.0 m wide and 10~12 m long 9%Ni steel plates. They are bent along the radius of curvature of the inner tank and erected by stacking 9 to 11 courses of the shell plates in the vertical direction. A recently constructed 200,000$m^3$ LNG storage tank used 24 plates with 3.7-m-wide and 11-m-long plates for each course and involved a total of 264 plates for 11 courses. Due to the specialized welding and inspection requirements for 9%Ni steel plates, it takes approximately 20 days to finish a single course.

Therefore, in order to shorten the construction period of the LNG storage tank, it is most effective to reduce the work in the field by reducing the number of plates and the number of courses by using wide and long plates. However, few mills manufacture 9%Ni steel plates, and in limited size. Thus, the contractors or researchers focused on reduction of outer tank construction by adopting precast or high strength materials (Hoyle *et al*. 2013, ARUP 2017, Kim *et al*. 2017).

Recently, a steel mill in Gwangyang, South Korea successfully manufactured 5-m-wide and 15-m-long 9%Ni steel plates for use in LNG inner tank shell. In this paper, the tensile and Charpy V-notch (CVN) impact tests were conducted for the wide and long 9%Ni steel, and the results were compared with the international standards, ASTM A553 (2017c) and EN 10028-4 (British Standard 2017). The flatness of the large plates was investigated to verify its applicability. A feasibility study was conducted to evaluate the use of the wide and long 9%Ni steel plate in the LNG storage inner tank shell involving designing, fabrication and mock-up erection. The 200,000$m^3$ LNG storage tank was parametrically designed with wide and long 9%Ni steel plates in accordance with API 620 (API 2013a) as shown in Fig. 2. Cost analysis was conducted in terms of 9%Ni steel plate, welding consumable, welding labor, and inspection. The 10-mm and 25-mm-thick plates were test fabricated involving from pretreatment to packing. The two 25-mm-

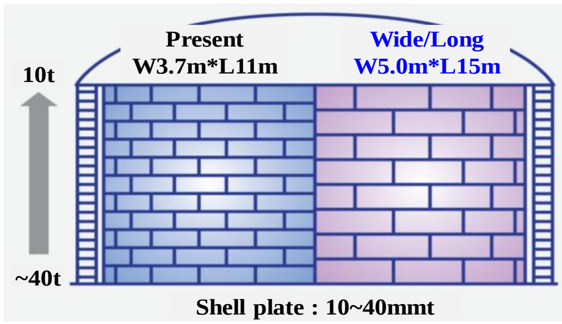


Fig. 2 Conceptual design of inner tank shell with wide and long plates

thick plates were erected to simulate stacking and welding of the wide and long plates. Based on the above procedure, the feasibility of the wide and long 9%Ni steel plate for use in the LNG storage inner tank shell was verified.

## 2. Characteristics of the wide and long 9%Ni steel plate

A low-carbon 9% Nickel alloy steel was developed more than 60 years ago for use in the structures that require ductility at temperature to –196℃. It attains high resistance subject to impact testing under cryogenic condition following appropriate heat treatment, QT (quenching and tempering) as shown in Fig. 3. Basically, the composition and manufacturing process of the wide and long 9%Ni steel plate is similar to that of 9%Ni steel reported previously except for varying heating and cooling details depending on the size, thickness, and the manufacturing environment.

Mechanical and chemical requirements for 9%Ni steel are specified in ASTM A553 (ASTM 2017c) and EN 10028-4 (British Standard 2017) as shown in Table 1. Both

(a) Heating

(b) Water quenching

(c) Correction

(d) Final shape (flat)

Fig. 3 Heat treatment and final shape of wide and long 9%Ni steel plate

standards specify thickness up to 50 mm, without indicating plate size. EN 10028-4 includes two groups varying in yield strength according to thickness, and the specific CVN values across 12 temperatures ranging from 20℃ to –196℃ while ASTM requires CVN values only at –195℃ (-320℉). EN 10028-4 requires averaged CVN values of 100 J and 80 J or larger for longitudinal and transverse directions, respectively, for the final plate rolling. According to ASTM A553, each impact test value shall constitute the average value of three specimens, with not more than one value below the specified minimum value of 34 J but in no case below 27 J for the full size 10 mm × 10 mm longitudinal specimens. Transverse specimens shall have the average value of three specimens, with not more than one value below the specified minimum value of 27 J but in no case below 20 J for the full size. Each test specimen shall have a lateral expansion opposite the notch of not less than 0.381 mm.

API 620 (API 2013a), that is a commonly used design and construction guideline for large, welded, low-pressure storage tanks, specifies the same CVN values and lateral expansion requirements as ASTM A553. However, it states that transverse specimens shall be tested for plates, including structural members made of plate, meanwhile, longitudinal specimens shall be tested for structural members. Retests shall be conducted in accordance with ASTM A353 (ASTM 2017a), A 553 (ASTM 2017c), and

Table 1 Mechanical property criteria for 9%Ni steel plate based on international standards

| | Grade | Thick (mm) | Chemical composition (%) | | | Y.S. (MPa) | T.S. (MPa) | Charpy V (–196℃) | |
|---|---|---|---|---|---|---|---|---|---|
| | | | C | Mn | Ni | | | Longi. | Transv. |
| ASTM A553 | Type I | ≤ 50 | ≤ 0.13 | ≤ 0.90 | 8.5~9.5 | 585 ≤ | 690~825 | 34J | 27J |
| EN 10028-4 | X7Ni9 | ≤ 30 | ≤ 0.10 | 0.3~0.8 | 8.5~10.0 | 585 ≤ | 680~820 | 100J | 80J |
| | | 30~50 | | | | 575 ≤ | | | |

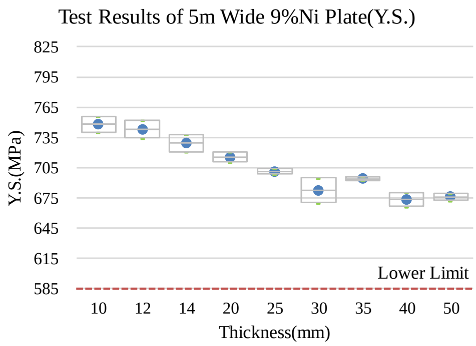


(a) Yield strength

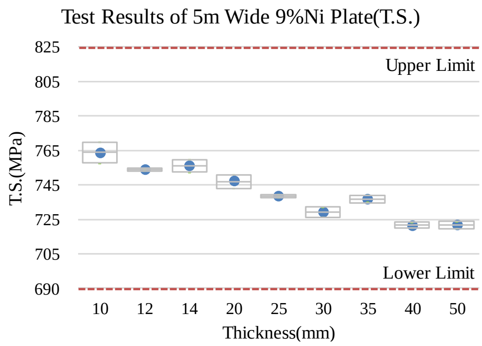


(b) Tensile strength

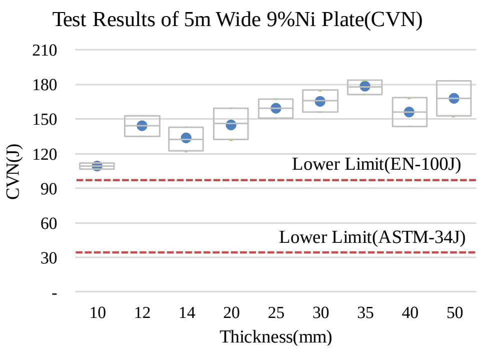


(c) Charpy energy for longitudinal specimens

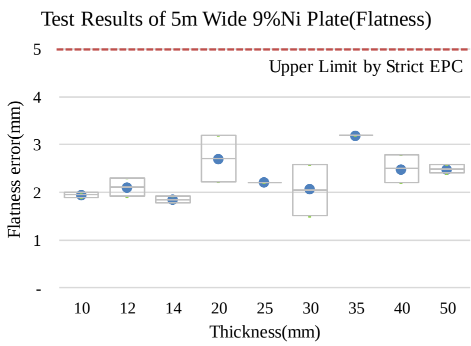


(d) Flatness

Fig. 4 Test and inspection results for the wide and long 9%Ni steel plate

A 645 (ASTM 2016) if any does not exceed the minimum values of 27 J and 20 J for longitudinal and transverse specimens. The above requirements are applicable to welded metal specimens as well.

The yield and tensile strengths resulting from the testing of the wide plates with a thickness ranging from 10 mm to 50 mm meet both standards with adequate margin as seen in Fig. 4. The thickness showed minimal deviation for both yield and tensile strengths. The average strengths decreased consistently with the increased thickness similar to the conventional steel. Similarly, the CVN values obtained from the test satisfied both standards. Flatness is a huge concern for wide and long plate that is vulnerable to local distortion due to unexpected and uneven cooling over the plate, and it could affect the tolerance control during erection. Therefore, EPC contractors stipulate strict flatness criteria requiring less than 5 mm. Fig. 4(d) verified that the flatness of wide and long 9%Ni steel plate after heat treatment could be controlled enough to satisfy the stringent EPC criteria regardless of thickness ranging from 10 mm to 50 mm. From the results above, the wide and long 9%Ni steel plates with thickness from 10 mm to 50 mm could be satisfactorily manufactured.

## 3. Fabrication of the wide and long 9%Ni steel plate

The 9%Ni steel plates are fabricated in a workshop before delivery to a construction site. The fabrication process includes pre-treatment, cutting, bevelling, roll bending, painting, packing as seen in Fig. 5 and followed by transportation.

Basically, the plates must not be in direct contact with the ground or other bundles. Plate clamps should be used without magnetism when loading and unloading the plates and have protective material in place to prevent the jaw ridges from coming into direct contact with the plates and indenting because 9%Ni steel is susceptible to magnetism. The lifting gear must not distort the shape of the plate during the lift as seen in Fig. 5. If possible, use of vacuum crane is recommended for transfer. Measurement of magnetic field strength of the plates is required before bevelling to trace and monitor the changes in gauss rating.

The plate edges are bevelled or squared as described in the contract drawing. The edges are sheared or machined; however, flame cutting is not preferred due to the sensitivity of heat-treated steel. Rolling and bending of the 9%Ni steel plate is similar to that of the conventional carbon steel except that extra care is needed to prevent magnetization. Both plate surfaces should be coated for ocean and water transport. In cases, the 9%Ni steel plate may be covered for ocean shipment without painting upon request by the contractor. The lifting or transferring should be conducted slowly and evenly. All bent plates are shipped with the plate ends supported on wooden skids, to maintain the radius of curvature.

The use of wide and long 9%Ni steel plate affects several fabrication steps and facilities. It requires larger facilities such as pre-treatment equipment, vacuum crane, and roll bender that can handle wider, longer and heavier plates. The sloping carriage of truck needs to be modified for land transportation. In this study, a larger capacity vacuum crane was installed in order to handle and fabricate larger plates up to 18 tons plates. The roll bender was renovated to handle up to 5 m wide plates as shown in


(a) General fabrication procedure

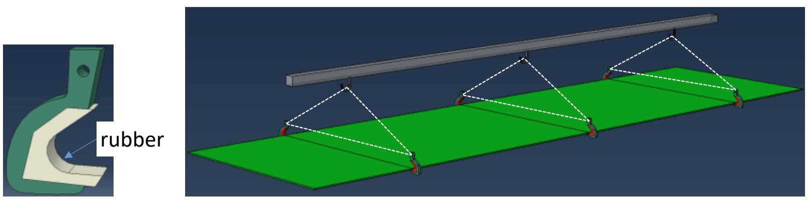


(b) Lifting gear and hook

Fig. 5 Procedure of 9%Ni steel plate fabrication

(a) 10 mmt, 4.8 m wide plate handling with vacuum crane

(b) Roll bending of 25 mmt, 4.5 m wide plate

(c) 10 mm, 4.8 m wide plate sloping carriage

Fig. 6 Facility renovation for handling and fabrication of wide and long 9%Ni steel plate

Fig. 6. For test fabrication, plates measuring 10 mm and 25 mm in thickness, 4.8~5.0 m in width, and 15 m in length, and manufactured in a steel mill were test fabricated. They resulted in final size of 4.5~4.8 m width and 14.8 m length due to taking specimens for welding test and some cutting loss. The 10-mm-thick plate was tested for handling, pre-treatment, bevelling. The 25-mm-thick plates were tested for additional processes including roll bending and truck transportation. The two 25-mm-thick plates were test erected to simulate stacking and welding similar to the

Fig. 7 Fabricated 25 mm, 4.5 m wide 9%Ni steel plate

construction site.

Tolerance to fabrication was investigated for length, width, diagonals, camber, bevel, plate curvature, and variation in the cylindrical surface perpendicular to the direction of rolling, such that the maximum difference in length was within 2 mm to 4 mm and 1 mm to 2 mm in length and width, respectively. The detailed specification is provided by each EPC contractor. Tolerance conditions similar to the previous smaller-sized plate was used to secure conservative fabrication precision. In the test fabrication, all the plates showed fabrication errors identical to conventional plates as illustrated in Fig. 7.

## 4. Erection of the wide and long 9%Ni steel plate

### *4.1 Verification for welding of wide and long 9%Ni steel plate*

Shielded metal arc welding (SMAW) in the 3G welding position is used for vertical welding of adjacent plates after the curved plates in the tank shell are placed circumferentially in each course. The plates in a course are horizontally welded to plates in the next course using SAW (submerged arc welding) with 2G welding position. 25-mm-thick steel plates taken from the wide and long plates were test welded using SMAW and SAW using the same welding consumables and procedures as in the site, then evaluated for tensile strength and toughness. Joint details such as groove angle, and root geometry for both types of welding are presented in Fig. 8. The base metal was backed with weld metal (W/M) but without a retainer. Root gaps and

Table 2 Welding condition of 9%Ni steel plates for SMAW and SAW

| | Pass No. | 1 | 2 | 3 | 4 | | B1 | B2 | B3 |
|---|---|---|---|---|---|---|---|---|---|
| | Process | SMAW with Φ4.0 mm filler metal, ENiMo-8(AWS classification) produced by KOBELCO Minimum preheat temperature 43℃, maximum inter-pass temperature 109℃ | | | | | | | |
| . | Amp. (A) | 140 | 127 | 107 | 110 | Back Gouging | 130 | 133 | - |
| | Volt (V) | 26 | 25 | 24 | 25 | | 25 | 26 | - |
| | Speed (CPM) | 6.06 | 4.44 | 8.33 | 6.89 | | 5.71 | 5.26 | - |
| | H/Input (KJ/cm) | 36.03 | 42.90 | 18.49 | 23.94 | | 34.15 | 39.44 | - |
| SAW | Pass No. | F1-F2 | F3 | F4-F5 | - | | B1 | B2 | B3 |
| | Process | SAW with Φ2.4 mm filler metal, ERNiMo-8(AWS classification) produced by KOBELCO Minimum preheat temperature 47℃, maximum inter-pass temperature 126℃ | | | | | | | |
| | Amp. (A) | 330 | 330 | 330 | - | Back Gouging | 330 | 330 | 330 |
| | Volt(V) | 29 | 29 | 29 | - | | 29 | 29 | 29 |
| | Speed(CPM) | 30.0-31.6 | 25.5 | 31.6 | - | | 31 | 29.6 | 31.3 |
| | H/Input (KJ/cm) | 18.17-19.14 | 22.51 | 18.17 | - | | 18.52 | 19.39 | 18.34 |

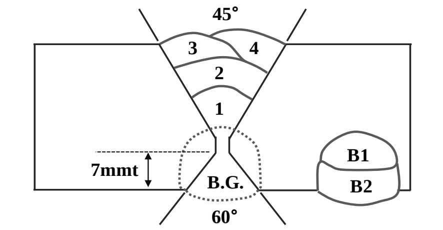


(a) Vertical SMAW welding

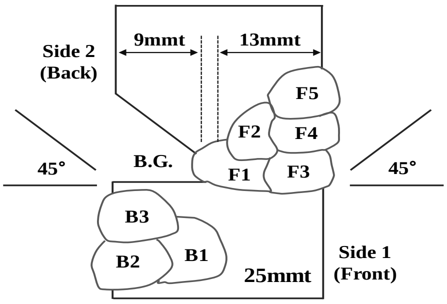


(b) Horizontal SAW welding

Fig. 8 Joint details for welding qualification

root faces for SMAW were 2 mm and 2 mm, respectively, and 1 mm and 3 mm for SAW, respectively. Detailed welding conditions are listed in Table 2.

Tensile and Charpy-V impact test results of the welded test specimens for SMAW and SAW are provided in Table 3. The tensile strengths of welded specimens were slightly lower than those of the base metal (Fig. 4). However, they all met the requisite tensile strength criteria ranging from 690 MPa to 825 MPa based on ASTM A553 (ASTM 2017c), and between 680 MPa and 820 MPa according to EN 10028-4 (2017). The failure was detected in the weld metal and ductile behaviour at failure was observed in all specimens.

The Charpy-V impact test is to investigate notch toughness, a measure of the metal's resistance to brittle fracture by a flaw or notch and fast loading conditions. The energy absorbed in fracture generally implies the notch toughness of the material, in addition, percent shear area and lateral expansion used to be a measure determining ductility (Manahan *et al*. 2018). The average energy absorbed from the impact test at –196℃ was 83.6 J and 144.6 J for W/M and HAZ, respectively, in SMAW, and 102.3 J and 177 J on average for W/M and HAZ, respectively, with SAW. This result may be attributed to the welding conditions such that SAW is automatically controlled under consistent and relatively low heat input.

A lateral expansion of 1.45 mm to 2.08 mm was observed for SMAW, and 0.81 mm to 1.22 mm with SAW. This indicates higher lateral deformation at the section of fracture in SMAW specimens compared with SAW, contrary to the results of absorbed energy. Therefore, lateral expansion might be a complementary parameter in determining ductility, but not the main criterion. Table 3 shows that almost every SMAW specimen failed by shear

Table 3 Tensile strength and toughness of 9%Ni steel plates for SMAW and SAW

| | | Specimen No. | Size (mm) | | Area ($mm^2$) | Ultimate load (kN) | Ultimate stress (MPa) | Type of failure & location |
|---|---|---|---|---|---|---|---|---|
| | | | Width | Thick | | | | |
| Tensile test | SMAW | T41 | 19.18 | 25.04 | 480.26 | 351.6 | 732 | Ductile at weld metal |
| | | T42 | 19.13 | 25.02 | 478.63 | 344.1 | 719 | Ductile at weld metal |
| | SAW | T21 | 18.8 | 24.5 | 460.6 | 326.6 | 709 | Ductile at weld metal |
| | | T22 | 18.8 | 24.4 | 458.7 | 317.4 | 692 | Ductile at weld metal |

| | | Specimen No. | Notch location | Notch type | Test temp. (℃) | Impact test (J) Ind. | Impact test (J) Avg. | Lateral expansion (mm) | Shear area (%) |
|---|---|---|---|---|---|---|---|---|---|
| Toughness test (10×10×55, in mm) | SMAW | W41 | W/M | 2-V | -196 | 89 | 83.6 | 1.79 | 100 |
| | | W42 | | | | 79 | | 1.45 | 95 |
| | | W43 | | | | 83 | | 1.53 | 100 |
| | | T41 | HAZ | 2-V | -196 | 153 | 144.6 | 2.08 | 100 |
| | | T42 | | | | 131 | | 1.79 | 100 |
| | | T43 | | | | 150 | | 1.91 | 100 |
| | SAW | W21 | W/M | 2-V | -196 | 100 | 102.3 | 0.85 | 50 |
| | | W22 | | | | 113 | | 0.88 | 40 |
| | | W23 | | | | 94 | | 0.81 | 50 |
| | | T21 | HAZ | 2-V | -196 | 197 | 177.0 | 1.22 | 40 |
| | | T22 | | | | 176 | | 1.16 | 40 |
| | | T23 | | | | 158 | | 1.08 | 40 |

(a) Erected two plates (b) SAW welding

Fig. 9 Erection of 25-mm-thick and 4.5-m-wide 9%Ni steel plates

and the percent shear areas at fracture ranged from 95% to 100%. However, SAW specimens showed 40% to 50% percent shear areas at fracture. If ductility measurement was based on the percent shear area, SMAW is inappropriate due to lack of ductility. Furthermore, the uncertainty of percent shear area measurement is at best 10% (Manahan *et al*. 2018). Therefore, the percent shear area criterion cannot be a specific parameter in ductility measurement.

### *4.2 Test erection of the wide and long 9%Ni steel plate*

In order to verify erection feasibility of the wide and long 9%Ni steel plate, two 25-mm-thick, 4.5-m-wide and 14.8-m-long 9%Ni steel plates were erected in a yard of plate fabrication workshop. A steel frame was fabricated to place and hold the curved wide and long plates as shown in Fig. 9 to simulate the actual erection process. To avoid the direct contact between carbon steel and 9%Ni steel, the possible contact points of steel were covered with rubber. The SAW welder carrier was hung over the top edge of the upper plate as illustrated in Fig. 9, which moves along the top edge for progressive welding of plates. In the study, the carrier was revamped to locate the welder at the exactly center of two wide plates. Welding consumable and welding conditions such as heat input and welding speed listed in Table 2, used in the actual construction, were used to weld the two erected plates. Based on the test fabrication, erection and inspection, no undesirable welding failure or deformation was observed. Witnesses from EPC contractors and engineering companies confirmed the handling, fabrication and erection feasibility.

## 5. Parametric design of 200,000m$^3$ LNG storage inner tank with wide and long 9%Ni steel plate

### *5.1 Design procedure of LNG storage inner tank and considerations for use of wide and long 9%Ni steel plate*

The design of LNG storage tank is based on several factors and considerations such as design method (allowable stress design, factorized strength design, limit state design, etc.), design liquid level, sloshing height of a contained liquid, type of anchorage system, size of plates supplied by steel plate manufacturers, material properties, site environments and so on.

The key factors include the design concept, applied load cases, operation and emergency condition, and seismic forces. Compliance with the specified design criteria is

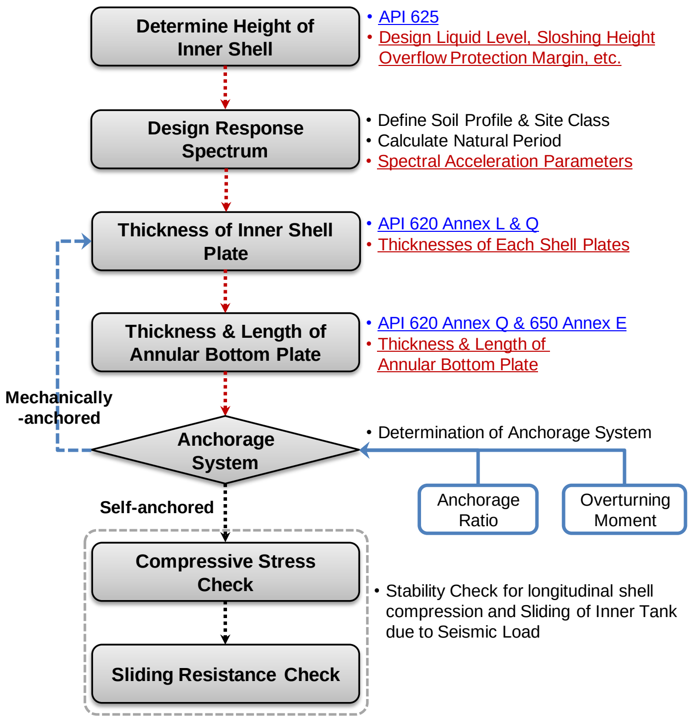


Fig. 10 Design procedure of LNG storage inner tank according to API 620 (API 2013a) & 625 (API 2010)

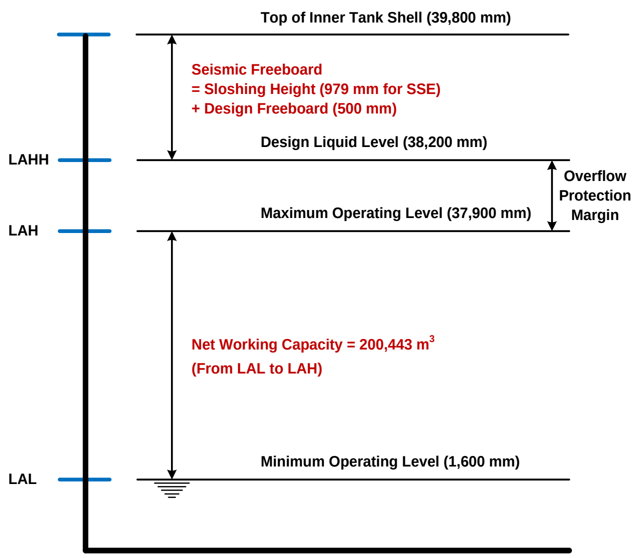


Fig. 11 Determination of design liquid level

essential to determine the dimension of inner tank. The criteria include tank height, and plate length, width, and thickness.

The procedure for the design of inner tank is described in Fig. 10. The diameter of LNG storage inner tank is determined by the value specified in a project document and the height is determined according to the design liquid level calculated from working capacity and content overflow protection, operation conditions, and seismic load as shown in Fig. 11. The thickness and width of each shell course are generally calculated according to the conditions of hydrostatic test and normal operation, and the stability of the inner tank should be verified under seismic condition.

### *5.1.1 Conditions of hydrostatic test and normal operation*

According to the API 620 requirements, the minimum thickness is 10 mm. The required shell thickness, $t$ is taken as the greater of the calculated thickness based on the following equations for normal operating (Eq. (1)) and hydrostatic test conditions (Eq. (2)).

$$t = \frac{R_c(\rho_L g H_d + P_g)}{S_{ts} E} + c = \frac{D(\rho_L g H_d + P_g)}{2 S_{ts} E} + c \tag{1}$$

$$t = \frac{R_c(\rho_w g H_t + P_g)}{S_{ts} E} + c = \frac{D(\rho_w g H_t + P_g)}{2 S_{ts} E} + c \tag{2}$$

in which, $D$ is the nominal tank diameter; $H_d$ denotes the height from the bottom of each course under consideration to the design liquid level; $H_t$ represents the height from the bottom of each course under consideration to the test water level; $\rho_L$ stands forr the density of LNG product; $\rho_w$ is the density of test water; $g$ denotes the acceleration of gravity; $P_g$ represents the design gas pressure and is equal to zero for inner tank with open top roof; $S_{ts}$ stands for the maximum allowable design stress determined in accordance with Q.3.3.2 of API 620 for normal operating condition; $E$ is the efficiency of welded joint (= 1.0 for butt joint); and $c$ is the corrosion allowance (= 0.0 mm).

### *5.1.2 Seismic condition*

The inner tank subjected to seismic load shall be designed and evaluated in accordance with API 620 Annex L. The inner tank and containment are considered as effective masses and the dynamic behavior of inner tank and its containment are theoretically obtained from API 650 Annex E (2013). According to API 650 Annex E, the seismic acceleration parameters of horizontal and vertical direction shall be defined by the design response spectra for OBE (operating basis earthquake) and SSE (safe shutdown earthquake) events based on the site-specific ground motion. The horizontal and vertical accelerations are applied together using the square root of sum of squares (SRSS) method.

The inner steel tank shall be designed to resist hoop tensile stresses due to the hydrostatic pressure and seismic forces. The dynamic hoop tensile stresses on inner shell plate due to seismic forces of OBE and SSE events shall be directly combined with the hoop stresses by hydrostatic pressure of the product in order to determine the total hoop stress as shown in the following equations. Here, the dynamic hoop stress is defined by the SRSS method of hoop tensile stresses for impulsive, convective and vertical forces

When the vertical acceleration is not considered

$$\sigma_T = \sigma_h + \sigma_s = \frac{N_h \pm \sqrt{N_i^2 + N_c^2}}{t} \tag{3}$$

When the vertical acceleration is specified

$$\sigma_T = \sigma_h + \sigma_s = \frac{N_h \pm \sqrt{N_i^2 + N_c^2 + (A_v N_h / 2.5)^2}}{t} \tag{4}$$

in which, $A_v$ is the vertical acceleration parameter; $N_h$ denotes the hydrostatic hoop force ($N/mm$); $N_i$ represents the impulsive hoop force defined in section E.6.1.4 of API 650 ($N/mm$); $N_c$ is the convective hoop force defined in section E.6.1.4 of API 650 ($N/mm$); $\sigma_T$ denotes the total hoop stress combined with hydrostatic and seismic forces ($MPa$); $\sigma_h$ stands for hydrostatic hoop stress ($MPa$); and $\sigma_s$ is hoop stresses due to impulsive and convective forces of the product ($MPa$).

### *5.1.3 Maximum allowable stresses*

The allowable stresses for hydrostatic test, normal operation, and seismic conditions shall be in accordance with API 620 Annex Q and L to determine the thicknesses and widths of each course of inner shell. The nominal strengths of 9%Ni steel plate and weld metal used in inner shell design are listed in Table 4.

The allowable stresses of 9%Ni steel plate are based on the lower yield and tensile strength of the weld metal and base metal. The maximum allowable design stresses are defined as the minimum of allowable stresses calculated for each design condition and are summarized in Table 5. The

Table 4 Nominal strength (MPa) of 9%Ni steel plate and weld metal

| | Yield strength ($\sigma_Y$) | Tensile strength ($\sigma_T$) |
|---|---|---|
| Base metal (9%Ni) | 585.0 | 690.0 |
| Weld metal | 399.9 | 690.0 |

Table 5 Maximum allowable stresses for each condition

| Condition | | Maximum allowable stresses |
|---|---|---|
| Hydrostatic test | | Min. [55% $\sigma_T$, 85% $\sigma_Y$ ] = 339.9 MPa |
| Normal operation | | Min. [1/3 $\sigma_T$, 2/3 $\sigma_Y$] = 230.0 MPa |
| Seismic | OBE | 133% of max. allowable stress for normal operation = 1.33 × 230.0 = 305.9 MPa |
| | SSE | |

nominal thickness, excluding corrosion allowance, is determined to satisfy all the maximum allowable stresses listed in the following table.

### *5.2 Parametric design of 200,000 m$^3$ LNG storage inner tank*

In recent years, 200,000 m$^3$ LNG storage tank was frequently designed and built. A preliminary design of an actual 200,000 m$^3$ LNG storage tank in Gwangyang, South Korea was selected as the basic model of parametric design. The diameter and height of inner tank shell were 84 m and 39.8 m, respectively. The shell consists of 11 courses of plates measuring 3.55 m to 3.65 m in width, and each course carries 24 curved plates circumferentially. In the parametric design, three width of 4.06 m, 4.44 m and 5.0 m were included, and a length of 14.7 m was assumed, which requires 18 plates to yield a circle with 84 m diameter. The plate length does not affect stress in plates because the stiffness of the tank shell is not changed by the length, so that the length change is only considered in the cost analysis. The thickness of each course for the cases was determined to satisfy API 620 and similar stress level as in the basic model. The results are presented in Table 6.

The structural design of tank shell is affected by the stiffness. If the stiffness remains similar to the basic model in the parametric design, the similar stress level could be obtained regardless of width of plates. Fig. 12 confirms that the thickness variation along the height of the shell is in a specified band. The lower vertices of the cases in Table 6 coincide in a line, however, slight differences between regression curves of each case is obtained for the upper vertices. The slopes of the linear regression curves are presented in Fig. 13, and a tendency of the value corresponding to plate width was obtained. Therefore, a simplified approach, that uses a regression curve of Figs. 12 and 13, might be used in the parametric design with respect to plate width variation. Once the thickness of the first course is determined, thickness of plates along the height of the shell can be computed using the slope determined from the regression equation in Fig. 13.

As the width increases from 3.65 m to 5.0 m, the number of courses could be decreased to 8 from 11.

Table 6 Tank shell design based on plate width

| Courses from bottom | Thickness, width of courses (mm) and hoop stress in inner shell plate (MPa) | | | |
|---|---|---|---|---|
| | Basic model | Case 1 | Case 2 | Case 3 |
| 1st | 34.0 / 3650 / 305.87 | 34.0 / 4060 / 305.87 | 34.0 / 4440 / 305.87 | 34.0 / 5000 / 305.87 |
| 2nd | 31.5 / 3650 / 305.70 | 31.2 / 4060 / 305.78 | 31.0 / 4440 / 305.06 | 30.5 / 5000 / 305.89 |
| 3rd | 28.9 / 3650 / 304.97 | 28.2 / 4060 / 305.82 | 27.5 / 4430 / 305.82 | 26.7 / 5000 / 305.88 |
| 4th | 26.0 / 3650 / 305.82 | 25.1 / 4060 / 304.79 | 24.0 / 4430 / 305.83 | 22.6 / 5000 / 305.31 |
| 5th | 23.1 / 3650 / 304.84 | 21.7 / 4060 / 304.97 | 20.3 / 4430 / 305.42 | 18.2 / 5000 / 304.95 |
| 6th | 19.9 / 3600 / 305.78 | 18.1 / 4060 / 305.34 | 16.4 / 4430 / 305.13 | 13.6 / 5000 / 305.15 |
| 7th | 16.7 / 3600 / 305.05 | 14.4 / 3860 / 303.91 | 12.2 / 4400 / 304.62 | 10.0 / 5000 / 268.07 |
| 8th | 13.3 / 3600 / 305.07 | 10.6 / 3860 / 304.52 | 10.0 / 4400 / 236.85 | 10.0 / 4800 / 109.01 |
| 9th | 10.0 / 3600 / 297.42 | 10.0 / 3860 / 202.77 | 10.0 / 4400 / 96.07 | - |
| 10th | 10.0 / 3600 / 184.63 | 10.0 / 3860 / 78.65 | - | - |
| 11th | 10.0 / 3550 / 68.72 | - | - | - |
| Total weight | 1,680 tonf | 1,691 tonf (+0.7%) | 1,701 tonf (+1.2%) | 1,711 tonf (+1.9%) |
| No. of plates | 264 | 180 (-31.8%) | 162 (-38.6%) | 144 (-45.5%) |

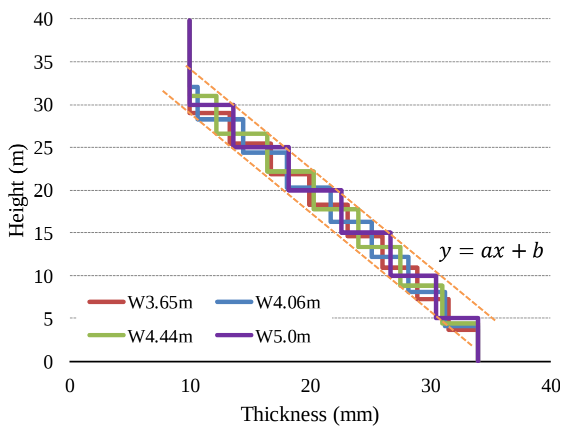


Fig. 12 Shell thickness variation along the height

Approximately 20 working days are needed to complete a course including placement, plate welding and inspection of welding by ultrasonic and radiographic methods. Therefore, the use of 5.0 m wide plate could reduce erection period by about 60 days in comparison with the basic model of 200,000 m$^3$ LNG storage tank. However, the wider plate increases the height of a course so that the total weight increase of steel plates is inevitable because thick plates

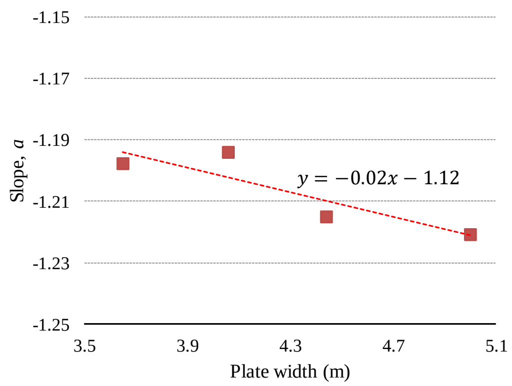


Fig. 13 Slopes of regression curves for upper vertices in Fig. 12 according to plate width

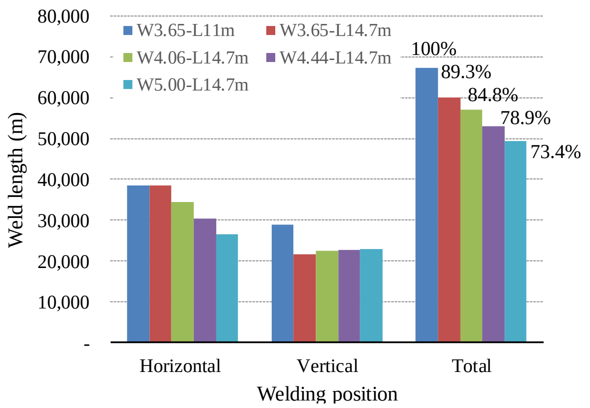


Fig. 14 Weld length of tank shell according to plate size

covers greater area as seen in Table 6. In the study, the weight increase ranged from 0.7% to 1.9% and the largest increase was observed in Case 2. The price of 9%Ni steel plate is 3 times or more expensive than conventional carbon steel, which hampered the economic benefit of the reduced erection period.

A rigorous analysis of the economic benefit was attempted based on a cost analysis of the main influencing cost factors such as welding consumables, welding labor and inspection. Cost of handling was assumed to be constant in all cases. In addition to the cases listed in Table 6, a modified basic model utilizing a 14.7-m-long plate with same width was considered. First, the weld length was calculated for all the cases. For comparison, the weld sizes of plates with varying thickness were converted into 6 mm, and the length was divided by deposition efficiency, 55% and 95% for SMAW and SAW, respectively (KOBELCO 2015). The results are presented in Fig. 14.

Increase in the plate length from 11 m to 14.7 m or decrease in the number of plates in a course from 24 to 18, decreased the vertical weld length in proportion to the decrease in the number of plates. Similarly, as the plate width increases from 3.65 m to 5.0 m or the number of courses decreases from 11 to 8, the horizontal weld length decreased approximately similar to the number of courses. The vertical weld accounts for 36% to 46% of the total weld length depending on the size of plates. As the plate length

Table 7 Cost analysis with respect to plate size

| | Cost (*1000USD) | | | | | | |
|---|---|---|---|---|---|---|---|
| | Basic model | | Modified model | Case 1 | Case 2 | Case 3 |
| Plate | 5,040 | 73.6% | 5,040 (-) | 5,074 (+0.7%) | 5,102 (+1.2%) | 5,133 (+1.9%) |
| Weld material | 333 | 4.9% | 297 (-10.7%) | 282 (-15.2%) | 263 (-21.1%) | 244 (-26.6%) |
| Weld labor | 1,346 | 19.7% | 1,202 (-10.7%) | 1,141 (-15.2%) | 1,062 (-21.1%) | 988 (-26.6%) |
| UT | 92 | 1.3% | 92 (-) | 83 (-10.0%) | 74 (-20.0%) | 65 (-30.0%) |
| RT | 36 | 0.5% | 27 (-25%) | 24 (-31.8%) | 22 (-38.6%) | 19 (-45.5%) |
| Total | 6,846 | 100% | 6,658 (-2.8%) | 6,605 (-3.5%) | 6,522 (-4.7%) | 6,450 (-5.8%) |

increased, the proportion decreased, and the proportion increased as the plate width increased. Thus, the modified basic model consisting of a 14.7-m-long plate with a width of 3.65 m exhibits the lowest vertical welding proportion of 36%. Case 3 showed the highest proportion of 46%. Basically, the vertically welded geometric length should be identical for all cases if the plate length is unchanged. Variations in thickness of the tank shell in each case yielded slight differences in welding volume and the normalized weld length as seen in Fig. 14. In summary, a mere increment of plate length from 11m to 14.7 m contributed to a 10.7% reduction in weld length. Increase in the plate length and width from W3.65 m × L11.0 m to W5.0 m × L14.7 m resulted in a 26.6% reduction in weld length.

In the cost analysis, the material, labor, inspection costs and conditions were assumed as follows:

(1) Prices of 9%Ni steel plate and welding material were $3,000/tonf and $35,000/tonf.
(2) Welding labor and equipment cost was $20/m.
(3) Cost of ultrasonic test along the circumferential welding line was $35/m.
(4) Cost of radiographic test was $135/plate.
(5) Cost that is not mentioned above was not considered.

Table 7 presents the results of cost analysis. In the basic model, the plates account for about 74% of total cost while the welding costs including material and labor accounted for about 25%. As shown in the results depicted in Table 7, the weight increase of tank shell with wider plates reached about 2%, suggesting that approximately 1.5% of the total cost was affected. Therefore, at least a reduction of 6% (1.5% = 25% × 6%) in welding cost is required to compensate for the increased plate weight. As seen in Fig. 14, the total weld length was reduced by 26.6% using the W5.0 m × L14.7 m plate, which directly contributed to the reduction of welding cost as shown in Table 7. Furthermore, a smaller number of plates led to further cost reduction in welding inspection. Considering all these economic effects, the use of 5.0-m-wide and 14.7-m-long 9%Ni steel plate for the construction of LNG storage tank shell yielded close to 6% in cost reduction. In addition to the direct cost effect, the construction period might be reduced by using a smaller number of plates.

## 6. Conclusions

In this paper, feasibility on the wide and long 9%Ni steel plate for use in the LNG storage inner tank shell was assessed in terms of material performance, fabrication, welding, erection, and economic benefit. The following conclusions were drawn through tests and parametric design:

(1) The tensile and Charpy V-notch(CVN) impact tests for the specimens taken from 5-m-wide and 15-m-long 9%Ni steel plates satisfied all the criteria by ASTM A553 (ASTM 2017c) and EN 10028-4 (British Standard 2017). Furthermore, flatness as small as 4 mm or less in the large plates was controlled satisfying the stringent requirements of EPC contractors.

(2) Plates measuring 10 mm and 25 mm in thickness, 4.8~5.0 m in width, and 15 m in length, and manufactured in a steel mill were test fabricated. They resulted in final size of 4.5~4.8 m width and 14.8 m length due to taking specimens for welding test and some cutting loss. The 10-mm-thick plate was tested for handling, pre-treatment, bevelling. The 25-mm-thick plates were tested for additional processes including roll bending and truck transportation. In the test fabrication, all the plates showed fabrication errors identical to those of conventional-sized plates.

(3) Tensile and Charpy-V impact test results of the welded test specimens for SMAW and SAW verified the performance of welded wide and long 9%Ni steel plates specified in API 620 (2013). The comparative test results confirmed that the absorbed energy from Charpy-V impact was the main parameter determining toughness and ductility rather than lateral expansion and percentage shear area.

(4) Erection feasibility of the wide and long 9%Ni steel plate was verified using the test erection of two 25-mm-thick, 4.5-m-wide and 14.8-m-long 9%Ni steel plates in a yard. Based on the test erection and inspection, no undesirable welding failure or deformation was observed. Witnesses from EPC contractors and engineering companies confirmed the handling, fabrication and erection feasibility.

(5) Parametric design using wide and long 9%Ni steel plates was carried out, and a simplified design method to determine the plate thickness along the shell height was proposed. The cost analysis based on the parametric design resulted in about 2% increase of steel weight; however, the construction cost was reduced about 6% due to large reduction in welding work.

## Acknowledgments

This study was financially supported by Seoul National University of Science & Technology.

## References

API (2010), API 625 - Tank Systems for Refrigerated Liquefied Gas Storage - First Edition, American Petroleum Institute, USA.

API (2013a), API 620 - Design and Construction of Large, Welded, Low-Pressure Storage Tanks – 12th Edition, American Petroleum Institute, USA.

API (2013b), API 650 - Welded Tanks for Oil Storage – 12th Edition, American Petroleum Institute, USA.

ARUP (2017), Gas and LNG Storage: The Future of Modular LNG Tanks; ARUP, UK.

ASTM (2016), ASTM A645 - Standard Specification for Pressure Vessel Plates, 5 % and 5.5 % Nickel Alloy Steels, Specially Heat Treated, ASTM International, USA.

ASTM (2017a), ASTM A353 - Standard Specification for Pressure Vessel Plates, Alloy Steel, Double-Normalized and Tempered 9 % Nickel, ASTM International, USA.

ASTM (2017b), ASTM A516 - Standard Specification for Pressure Vessel Plates, Carbon Steel, for Moderate- and Lower-Temperature Service; ASTM International, USA.

ASTM (2017c), ASTM A553 - Standard Specification for Pressure Vessel Plates, Alloy Steel, Quenched and Tempered 7, 8, and 9 % Nickel, ASTM International, USA.

Bouknight, H. (2015), *LNG Storage Solutions*: *A Key Consideration and Element in LNG Terminal Operation*, IHI, Japan.

British Standard (2017), EN 10028-4 - Flat products made of steels for pressure purposes. Part 4: Nickel alloy steels with specified low temperature properties, British Standards Institution, UK.

CLP Power (2006), Tank Technology Selection Study for the Hong Kong LNG Terminal; Tank Technology Study by CLP Power, Hong Kong.

Hjorteset, K., Wernli, M., NaNier, M.W., Hoyle, K.A. and Oliver, W.H. (2013), "Development of large-scale precast, prestressed concrete liquefied natural gas storage tanks", *PCI J*., **58**(4), 40-54. https://doi.org/10.15554/pcij.09012013.40.54

Hoyle, K., Oliver, S. and Tsai, N. (2013), "Composite Concrete Cryogenic Tank (C3T): A Precast Concrete Alternative for LNG Storage", *Proceedings of 17th International Conference & Exhibition on Liquified Natural Gas*, Houston, TX, USA.

IGU (2017), 2017 World LNG Report; International Gas Union, Spain.

Khamehchi, E., Yousefi, S.H. and Sanaei, A. (2013), "Selection of the Best Efficient Method for Natural Gas Storage at High Capacities Using TOPSIS Method", *Gas Process. J*., **1**(1), 9-18.

Kim, J.H., Lee, S.K., Lee, K.W., Oh, S.H., Jo, H.C. and Lim, Y.M. (2017), "Development of Fast Construction Method of LNG Storage Tank Wall Using Permanent Precast Concrete Form", *Proceedings of the 27th International Ocean and Polar Engineering Conference*, San Francisco, CA, USA.

KOBELCO (2015), The ABC's of Arc Welding and Inspection, KOBE STEEL, LTD, Japan.

Lee, S.W., Choi, S.J. and Kim, J.H. (2016a), "Analytical study of failure damage to 270,000-kL LNG storage tank under blast loading", *Comput. Concrete*, *Int. J*., **17**(2), 201-214. https://doi.org/10.12989/cac.2016.17.2.201

Lee, S., Seo, Y., Lee, J. and Chang, D. (2016b), "Economic evaluation of pressurized LNG supply chain", *J. Natural Gas Sci. Eng*., **33**, 405-418. https://doi.org/10.1016/j.jngse.2016.05.039

Manahan, M.P. Jr., McCowan, C.N. and Manahan, M.P. Sr. (2018), "Percent Shear Area Determination in Charpy Impact Testing", *J. ASTM Int.*, **5**(7), https://doi.org/10.1520/JAI101662

Nishigami, H., Kusagawa, M., Yamashita, M., Kawabata, T., Kamo, T., Onishi, K., Hirai, S., Sakato, N., Mitsumoto, M. and Hagihara, Y. (2012), "Development and realization of large scale LNG storage tank applying 7% Nickel steel plate", *Proceedings of World Gas Conference*, Kuala Lumpur, Malaysia.

Panchal, V.R. and Soni, D.P. (2014), "Seismic Behaviour of Isolated Fluid Storage Tanks: A-state-of-the-art Review", *KSCE J. Civil Eng.*, **18**(4), 1097-1104. https://doi.org/10.1007/s12205-014-0153-7

Sun, J., Cui, L., Li, X., Wang, Z., Liu, W. and Lv, Y. (2019), "Design theory and method of LNG isolation", *Earthq. Struct.*, **16**(1), 1-9. https://doi.org/10.12989/eas.2019.16.1.001

Yang, J. and Yang, G. (2014), "The temperature field research for large LNG cryogenic storage tank wall", *Appl. Mech. Mater.*, **668-669**, 733-736. https://doi.org/10.4028/www.scientific.net/AMM.668-669.733

*BU*